Detailed investigation of the superconducting transition of niobium disks exhibiting the paramagnetic Meissner effect

L. Půst and L. E. Wenger
Department of Physics and Astronomy, Wayne State University, Detroit, Michigan 48202

M. R. Koblischka
SRL/ISTEC, 1-16-25 Shibaura, Minato-ku, Tokyo 105, Japan

(Received 2 July 1998)

The superconducting transition region in a Nb disk showing the paramagnetic Meissner effect (PME) has been investigated in detail. From the field-cooled magnetization behavior, two well-defined temperatures can be associated with the appearance of the PME: T_1 ($<T_c$) indicates the characteristic temperature where the paramagnetic moment first appears and a lower temperature T_p ($<T_1$) defines the temperature where the positive moment no longer increases. During the subsequent warming, the paramagnetic moment begins to decrease at T_p and then vanishes at T_1 with the magnitude of the magnetization change between these two temperatures being nearly the same as that during cooling. This indicates that the nature of the PME is reversible and not associated with flux motion. Furthermore, the appearance of this paramagnetic moment is even observable in fields as large as 0.2 T even though the magnetization does not remain positive to the lowest temperatures. Magnetic hysteresis loops in the temperature range between T_1 and T_p also exhibit a distinct shape that is different from the archetypal shape of a bulk type-II superconductor. These behaviors are discussed in terms of the so-called ''giant vortex state.'' [S0163-1829(98)01945-6]

A fundamental property of superconductivity is the Meissner effect, i.e., the occurrence of flux expulsion below the superconducting transition temperature T_c and the resulting diamagnetic response to the applied magnetic field. In contrast to this behavior, several groups[1–7] have reported a ''paramagnetic'' signal when cooling certain samples of high-T_c superconductors [mainly $Bi_2Sr_2CaCu_2O_{8+\delta}$ ceramics, but also $Bi_2Sr_2Ca_2Cu_3O_{10+\delta}$ powder,[3] $YBa_2Cu_3O_{7-\delta}$ single crystals,[6] and $Nd_{2-x}Ce_xCuO_y$ (Ref. 7)] in magnetic fields smaller than 0.1 mT through T_c. This effect is now referred to as the paramagnetic Meissner effect (PME) or Wohlleben effect.

Several explanations for the origin of the PME have been given so far, including the formation of spontaneous currents due to π contacts[3] and spontaneous polarized orbital currents.[8] Furthermore, it has been argued that this effect is a consequence of *d*-wave superconductivity.[9] However, it still remains an open question why all high-T_c samples do not exhibit the PME.

The observation of a strikingly similar PME signal in disks of Nb,[10,11] which is an isotropic *s*-wave (BCS) superconductor, revived the discussion about the origin of the PME.[12] In turn, models based on flux trapping effects were proposed by Koshelev and Larkin (KL)[13] and Moshchalkov *et al.*[14] Since the microstructure of all high-T_c samples exhibiting the PME is complicated by the presence of granularity, misorientation of grains,[15] intrinsic Josephson junctions,[16] and the two-dimensional character resulting from the layered crystalline structure,[17] Nb may serve as an ideal system to clarify the mechanism responsible for the formation of a paramagnetic moment during field-cooling for both conventional and high-T_c superconducting samples.

In order to provide a deeper insight into the transition regime of Nb, detailed magnetic investigations have been performed in the field-cooled cooling (FCC) and field-cooled warming (FCW) modes. The results of the present investigation suggest that the common picture of the PME has to be revised. The field-cooled magnetization results for Nb disks show a paramagnetic moment that has a *reversible* nature as it appears and disappears at the same temperature T_1 ($<T_c$) during cooling and warming, respectively. This moment is superimposed on a typical diamagnetic superconducting behavior below T_1 and continues to increase in magnitude until the temperature, T_p ($<T_1$). Thus, the appearance of a net positive signal at lower temperatures depends on the relative magnitude of the paramagnetic moment of the sample to that of the diamagnetic moment below the temperature T_p.

Nb disks of diameter 6.4 mm were punched from 0.127-mm thick sheets (99.8% purity).[18] Each disk was then positioned at the center of the second-order gradiometric detector coil in a commercial SQUID magnetometer[19] with magnetic fields below 1 mT generated by a Cu solenoid which is part of its ultralow-field option. To avoid any residual flux trapped in the surrounding superconducting magnet, the entire magnet system was warmed above its superconducting transition temperature and the superconducting magnet was never energized until the completion of all measurements below 1 mT. During both temperature and field measurements the sample was kept stationary, thereby eliminating any spurious signals that might have arisen from field inhomogeneities with sample position. The analog voltage output from the SQUID amplifier, which is proportional to the magnetic flux change through the pickup coils, was then recorded continuously during the temperature scan and transformed into magnetic moment values. A nominal temperature sweep rate of 35 mK/min for both cooling and the sub-

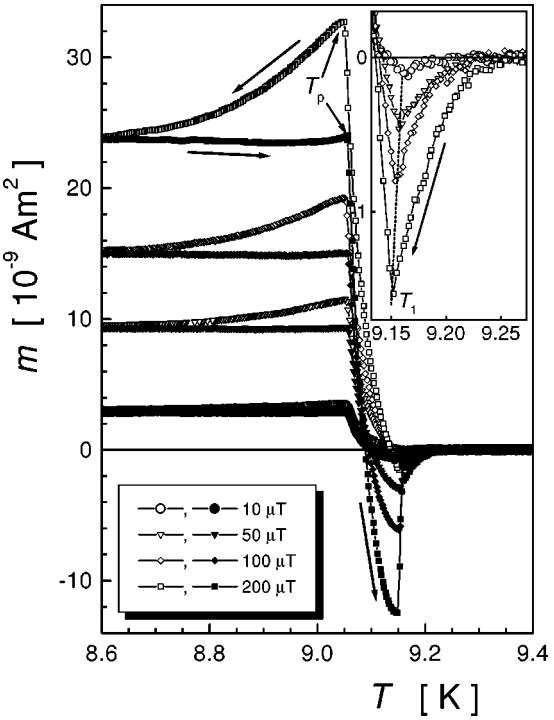

FIG. 1. Low-field field cooled $m(T)$ curves recorded during cooling (FCC: open symbols) and warming (FCW: solid symbols) on sample NbD4S2 in various fields $\mu_0 H_{ext}=10$ μT (circles), 50 μT (triangles), 100 μT (diamonds), and 200 μT (squares). The sharp, downward turn in the $m(T)$ curve corresponds to $T_p = 9.05$ K. Inset: Details of FCC curves just below the critical temperature indicating sharp turn towards positive values at temperature T_1. T_1 at various fields is indicated by a dashed line.

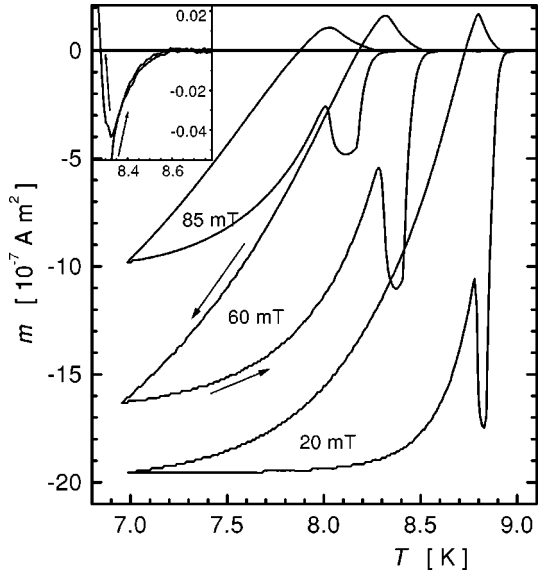

FIG. 2. FCC and FCW $m(T)$ curves recorded on sample NbD4S2 in fields $\mu_0 H_{ext}=20$, 60, and 85 mT. Note the significant step on the FCC curve towards positive values and the complementary step towards negative values on the FCW curve. Inset: Details of the curves at 85 mT with onset of diamagnetic moment at 8.6 K followed by a very sharp onset of a positive step on the FCC curve at $T_1=8.32$ K.

sequent warming was achieved by direct low-level control of the heaters in the system using the EDC option.[19] During magnetic-hysteresis-loop (MHL) measurements, the SQUID voltage component arising solely from the magnetic field sweep was subtracted from the measured voltages. The results presented in this communication are for one particular Nb disk (NbD4S2), see also Ref. 10.

Figure 1 presents detailed magnetic moment $m(T)$ results in the superconducting transition region for field-cooled cooling and field-cooled warming modes in magnetic fields between 10 and 200 μT. The temperature was continuously swept from 9.4 down to 8.5 K and then the temperature sweep direction is reversed. These scans of the magnetic moment $m(T)$ reveal several characteristic temperatures. T_c defines the onset of superconductivity and of a diamagnetic moment, which occurs at $\approx$9.23 K as shown in the inset of Fig. 1. Below T_c, $m(T)$ becomes more negative upon cooling until T_1 ($\approx$9.16 K at the lowest fields) where $m(T)$ abruptly turns towards positive values. This increase in $m(T)$ continues until another characteristic temperature T_p ($\approx$9.16 K at the lowest fields), is reached where $m(T)$ exhibits a cusplike behavior. Below T_p, the relative temperature dependence of $m(T)$ appears to correspond to the archetypal FCC behavior of a superconducting sample not exhibiting the PME. As discussed in Ref. 10, another characteristic feature of the PME for the Nb disks is the large hysteresis between the FCC and FCW curves with the FCW curves being lower than the FCC curves. Upon warming, the $m(T)$ curves remain practically constant until the moment turns abruptly towards negative values at a temperature essentially the same as T_p. Then, at a temperature identical to T_1, $m(T)$ jumps to a less diamagnetic and more probable equilibrium value as the PME appears to suddenly vanish. The similarity in characteristic temperatures where the positive moment first appears during cooling and then disappears during warming as well as where the positive contribution stops increasing in magnitude during cooling and subsequently begins to decrease upon warming suggests that the PME has a reversible nature.

The same basic features can even be observed in the FCC and FCW curves recorded at magnetic fields as high as 0.2 T. In Fig. 2 the $m(T)$ behaviors are presented for applied fields from 20 to 85 mT. The onset of diamagnetism just below T_c in the FCC curves is still present as illustrated in the inset for a field of 85 mT. The onset of a diamagnetic moment at $T_c = 8.6$ K is followed by a very sharp positive rise in the FCC curve at $T_1=8.32$ K which eventually reaches a maximum at T_p. However, instead of remaining positive for all temperatures below T_p as in the low-field measurements, the overall $m(T)$ becomes diamagnetic which suggests that the diamagnetic component outweighs the paramagnetic component at these higher fields. Nevertheless, the paramagnetic component is still present in the sample at $T \ll T_p$ as evidenced by the corresponding FCW curves. Even though $m(T)$ during FCW is always diamagnetic up to T_c, there is a noticeable change towards larger diamagnetic values at a temperature very close to T_p followed by a jump towards a vanishingly small $m(T)$ value at a temperature similar to T_1 (see inset). With decreasing magnetic field, this jump becomes increasingly less broad and eventually becomes discontinuous at the lowest fields. This characteristic behavior associated with the appearance and disappearance of the positive moment even

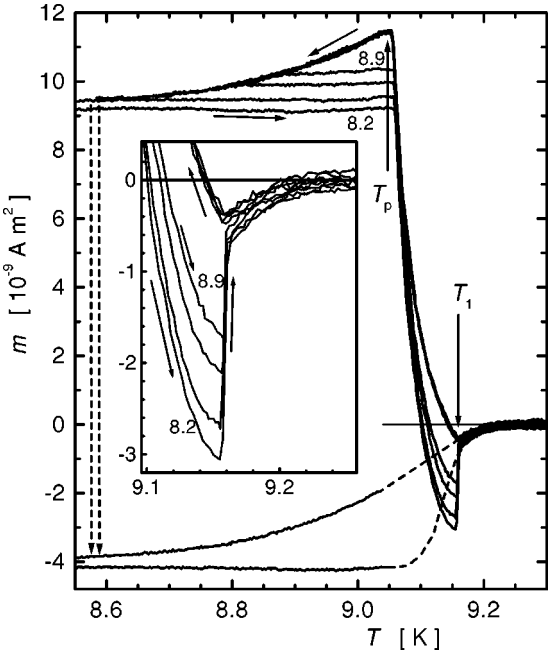

FIG. 3. FCC and FCW $m(T)$ curves for a constant field $\mu_0 H_{\rm ext}=50$ μT measured down to various $T_{\rm min}<T_p$. To estimate the magnitude of the paramagnetic step on the FCC and FCW curves, both curves below T_p are shifted by $m_{\rm shift}=1.33\times10^{-9}$ Am^2 (dashed lines) to such a position that $m(T)$ above T_1 and below T_p point toward each other. Inset: Details of FCC and FCW curves around T_1.

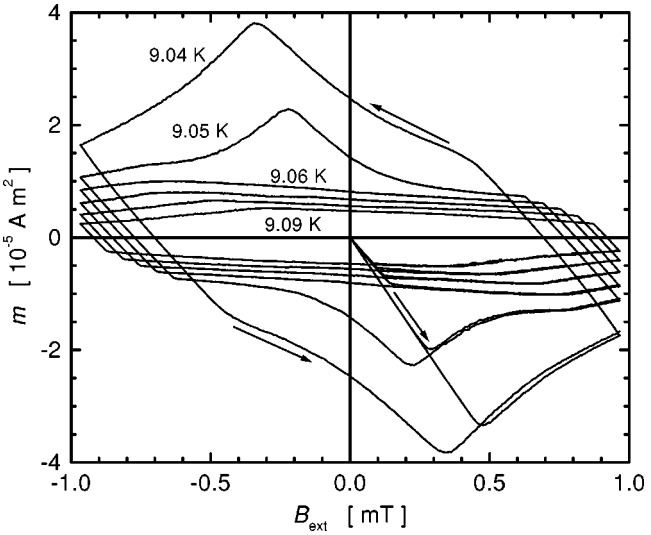

FIG. 4. Magnetic hysteresis loops (MHL) in the temperature range $9.04\leqslant T\leqslant 9.09$ K for 0.01 K increments. Note the remarkable change of the MHL shape between 9.05 and 9.06 K, i.e., at $T=T_p$.

in high fields gives further credence to the reversible nature of the PME.

Figure 3 further illustrates the reversible nature of the paramagnetic component of the magnetic moment. While the field is kept fixed at $\mu_0 H_{\rm ext}=50$ μT, the temperature is cooled to various temperatures $T_{\rm min}(<T_p)$ and then subsequently raised above T_c. While all FCC curves overlap as expected, the FCW curves below T_p are nearly temperature independent with the magnitude being dependent upon $T_{\rm min}$. Above T_p, $m(T)$ during FCW decreases rapidly until T_1. Just below T_1, $m(T)$ jumps abruptly towards a value close to that of the FCC curve suggesting that the FCC curves above T_1 are in equilibrium. The size of this jump at $T=T_1$ depends only on the moment value at the onset of the step at T_p. Further note that the shape and size of the change in $m(T)$ between T_p and T_1 are nearly the same for all warming curves with each $m(T)$ curve being shifted downwards for lower $T_{\rm min}$. Even the complementary FCC curves appear to have a similar shape and magnitude change in this temperature region suggesting the paramagnetic component is nonhysteretic.

To estimate the separate paramagnetic and diamagnetic components, the PME contribution is assumed to be constant below T_p. The resulting FCC and FCW data below T_p are then shifted by $m_{\rm shift}=1.33\times10^{-9}$ Am^2 as shown in Fig. 3 for the $T_{\rm min}=8.2$ K data. The resulting ''shifted'' curves with the interpolations between T_1 and T_p (dashed lines) appear to form FCC and FCW curves for a archetypal type-II superconductor. Thus the characteristic $m(T)$ behavior can be regarded as consisting of two additive moments: a hysteretic behavior arising from the flux trapping and diamagnetic screening associated with a typical type-II superconducting sample and a *nearly reversible* behavior associated with the PME of the sample which appears and disappears at a well-defined temperature of T_1. At low fields, the abrupt appearance (disappearance) of this positive moment upon cooling below T_1 (warming just below T_1) is fairly spontaneous similar to the onset (disappearance) of global diamagnetic screening currents at T_c rather than the viscous nature exemplified by flux flow. Below T_p, this moment apparently does not change with temperature and can be regarded as an additive constant to the field-cooled magnetic moment of a non-PME superconductor.

To gain further insight into the nature of this additive paramagnetic moment for the Nb disks, magnetic hysteresis loops (MHLs) were measured. A set of MHLs recorded in the temperature range from 9.04 to 9.09 K, i.e., around T_p, are presented in Fig. 4. The MHLs between T_1 and T_p are found to exhibit several distinct features which probably have the same physical origin as the appearance of the paramagnetic moment during cooling in small applied fields. Between T_c and T_1, the sample is superconducting, but only a small diamagnetic screening current can be induced by ramping $H_{\rm ext}$. Below T_1, the magnitude of the critical currents increases significantly, and the MHLs exhibit a strange, nearly parallelogramlike shape. Note that the reverse legs are entirely linear, all ''corners'' are quite sharp, and the size of the parallelograms increases with decreasing temperature. Also, the shape of the initial curves is very linear and merges with the loop quite abruptly. Just below T_p, a remarkable change in the shape of the MHLs takes place as the MHLs acquire the archetypal behavior for a bulk type-II superconductor with a maximum close to $H_{\rm ext}=0$. Additionally, the slope $dm/dH_{\rm ext}$ of the initial curves changes by about 20% below T_p with the magnitude of this change corresponding to the step observed in the zero field-cooled magnetization curves.[10]

As reported previously, the sample surface plays a crucial role in the appearance of the paramagnetic moment in the Nb

disk sample. These PME effects were found to vanish after mechanical abrading the disk's top and bottom surfaces and reducing the overall thickness by about 10% (Refs. 10,11) while a net positive magnetic moment was induced into a thicker Nb disk by means of ion implanting.[21] Neither the simple approach of flux compression by KL (Ref. 13) nor the incorporation of the surface effects[11] seems to explain the features reported here. However, our measurements appear to be more consistent with a superconducting current forming a large ''giant vortex'' on the sample surface. Giant vortex states were first described theoretically by Fink and Presson[22] and more recently as a possible source for the PME by Moshchalkov *et al.*[14] The basic premise is that the giant vortex state with a fixed orbital quantum number is formed as the superconductor is field cooled at the third (surface) critical field $H_{c3}(T)$. With decreasing temperature, the superconducting order parameter would grow and compress the trapped flux into a giant vortex leading to a positive or paramagnetic response. However, the original model pictured a single giant vortex developing from the edges of a cylindrical sample as compared to several individual vortices developing at microstructural defects on the disk's surface. Thus it is important to determine the flux and/or screening current distributions in samples exhibiting the PME in the transition region between T_1 and T_p. Using highly sensitive imaging techniques,[20] e.g., could clarify the origin of the PME in Nb as well as elucidate our understanding of the PME in high-T_c superconductors. In granular samples, the surface of the individual grains may have deteriorated thus providing a similar surface layer with different superconducting properties as on our Nb disk surfaces.

In summary, the present measurements suggest that the nature of the PME is reversible and not associated with flux motion as the total magnetization consists of two components: a nearly reversible positive moment superimposed on a hysteretic diamagnetic superconducting behavior below T_1. Consequently, the appearance of a net positive signal at lower temperatures depends on the relative magnitude of the diamagnetic moment of the sample to that of the paramagnetic moment.

L.P. and L.E.W. acknowledge support from NATO Grant No. 961357 while M.R.K. was supported by STA.

[1] P. Svedlindh, K. Niskanen, P. Norling, P. Nordblad, L. Lundgren, B. Lönnberg, and T. Lundström, Physica C **162-164**, 1365 (1989).

[2] W. Braunisch, N. Knauf, V. Kataev, S. Neuhausen, R. Grütz, B. Roden, D. Khomskii, and D. Wohlleben, Phys. Rev. Lett. **68**, 1908 (1992).

[3] W. Braunisch, N. Knauf, G. Bauer, A. Kock, A. Becker, B. Freitag, R. Grütz, V. Kataev, S. Neuhausen, B. Roden, D. Khomskii, D. Wohlleben, J. Bock, and E. Preisler, Phys. Rev. B **48**, 4030 (1993).

[4] J. Kötzler, M. Baumann, and N. Knauf, Phys. Rev. B **52**, 1215 (1995).

[5] Ch. Heinzel, Th. Theilig, and P. Ziemann, Phys. Rev. B **48**, 3445 (1993).

[6] S. Riedling *et al.*, Phys. Rev. B **49**, 13 283 (1994); R. Lucht, H. v. Löhneysen, H. Claus, M. Kläser, and G. Müller-Vogt, *ibid.* **52**, 9724 (1995).

[7] G. S. Okram, D. T. Adroja, B. D. Padalia, O. Prakash, and P. A. J. de Groot, J. Phys. C **9**, L525 (1997).

[8] F. V. Kusmartsev, Phys. Rev. Lett. **69**, 2268 (1992).

[9] T. M. Rice and M. Sigrist, J. Phys. Soc. Jpn. **62**, 4283 (1992); Rev. Mod. Phys. **67**, 503 (1995).

[10] D. J. Thompson, M. S. M. Minhaj, L. E. Wenger, and J. T. Chen, Phys. Rev. Lett. **75**, 529 (1995).

[11] P. Kostić, B. Veal, A. P. Paulikas, U. Welp, V. R. Todt, C. Gu, U. Gaiser, J. M. Williams, K. D. Carlson, and R. A. Klemm, Phys. Rev. B **53**, 791 (1996).

[12] T. M. Rice and M. Sigrist, Phys. Rev. B **55**, 14 647 (1997); P. Kostić *et al.*, *ibid.* **55**, 14 649 (1997).

[13] A. E. Koshelev and A. I. Larkin, Phys. Rev. B **52**, 13 559 (1995).

[14] V. V. Moshchalkov, X. G. Qiu, and V. Bruyndoncx, Phys. Rev. B **55**, 11 793 (1997).

[15] J. R. Clem, Physica C **153-155**, 50 (1988); M. V. Feigel'man and L. B. Ioffe, Phys. Rev. Lett. **74**, 3447 (1995).

[16] M. Rapp, A. Murk, R. Semerad, and W. Prusseit, Phys. Rev. Lett. **77**, 928 (1996).

[17] D. Feinberg and D. Villard, Phys. Rev. Lett. **65**, 919 (1990); E. H. Brandt, *ibid.* **66**, 3213 (1991).

[18] Johnson-Mattey Inc., Seabrook, NH 03874.

[19] Quantum Design, San Diego, CA 92121, model MPMS5S with ultra-low-field option.

[20] For the direct imaging of the giant vortex state, the scanning SQUID technique, see, e.g., J. R. Kirtley, C. C. Tsuei, M. Rupp, J. Z. Sun, L. S. Yu-Jahnes, A. Gupta, M. B. Ketchen, K. A. Moler, and M. Bushan, Phys. Rev. Lett. **76**, 1336 (1995), or the micro-Hall probe technique, see, e.g., M. Konczykowski, F. Holtzberg, and P. Lejay, Supercond. Sci. Technol. **4**, S445 (1991), may be employed.

[21] D. J. Thompson, L. E. Wenger, and J. T. Chen, Phys. Rev. B **54**, 16 096 (1996).

[22] L. J. Barnes and H. J. Fink, Phys. Rev. **149**, 186 (1966); Phys. Lett. **20**, 583 (1966); H. J. Fink and X. Presson, Phys. Rev. **151**, 219 (1966).